

Enhancing Sequential Model Performance with Squared Sigmoid TanH (SST) Activation Under Data Constraints

Barathi Subramanian*, Rathinaraja Jeyaraj**, Rakhmonov Akhrorjon Akhmadjon Ugli*, and Jeonghong Kim*

*Kyungpook National University, Daegu, South Korea

**University of Huston-Victoria, Texas, USA

Abstract – Activation functions enable neural networks to learn complex representations by introducing non-linearities. While feedforward models commonly use rectified linear units, sequential models like recurrent neural networks, long short-term memory (LSTMs) and gated recurrent units (GRUs) still rely on Sigmoid and TanH activation functions. However, these classical activation functions often struggle to model sparse patterns when trained on small sequential datasets to effectively capture temporal dependencies. To address this limitation, we propose squared Sigmoid TanH (SST) activation specifically tailored to enhance the learning capability of sequential models under data constraints. SST applies mathematical squaring to amplify differences between strong and weak activations as signals propagate over time, facilitating improved gradient flow and information filtering. We evaluate SST-powered LSTMs and GRUs for diverse applications, such as sign language recognition, regression, and time-series classification tasks, where the dataset is limited. Our experiments demonstrate that SST models consistently outperform RNN-based models with baseline activations, exhibiting improved test accuracy.

Keywords – Activation function, GRU, Sigmoid, TanH

1. Introduction

In deep learning, activation functions (AFs) play a crucial role in neural networks by introducing non-linearities, enabling them to learn complex patterns in data [1]. An AF essentially decides whether a neuron should be activated or not, by calculating a weighted sum and further adding bias to it. Ideal AFs should meet additional criteria other than non-linearity such as facilitating convergence during network training, minimizing computational complexity, promoting smooth gradient flow, and preserving data distribution criteria to enhance training effectiveness [2]. Common AFs include linear or identity, where output is proportional to the input. Non-linear functions like Sigmoid and Hyperbolic Tangent (TanH), which normalize output within a range; and rectified linear unit (ReLU) [3] and its variants like Leaky ReLU [4] and Parametric ReLU [5], which have been effective in mitigating the vanishing gradient problem in deep networks. Each of these functions has distinct characteristics and is chosen based on the specific requirements of the neural network and the complexity of the data it handles.

Despite their wide usage, these AFs have limitations, especially in sequential data applications with recurrent neural networks (RNN) like long short-term memory (LSTMs) and gated recurrent units (GRUs) [6-9]. Saturating activations like Sigmoid and TanH are prone to vanishing gradient problems, which hinder the network's ability to learn from data, particularly in deep networks or when dealing with long sequences [6, 10]. ReLU and its variants, while addressing some of these issues in feedforward networks, are not always optimal for sequential models as they can lead to dead neurons or exploding gradient problems [11-13]. These limitations become more pronounced in scenarios involving small dataset, where the network struggles to effectively model temporal dependencies and generalize [14] due to sparse pattern in the dataset.

To address these challenges, we introduce the Squared Sigmoid and TanH (SST) AF. SST squares the output of the Sigmoid and TanH AFs. This approach amplifies the differences between strong and weak activations, enhancing gradient flow and information filtering as signals propagate through time in sequential models. Especially, SST offers advantages in improving memory and learning for GRU, which is highly preferred while dealing with limited dataset. By squaring the Sigmoid and TanH outputs, SST increases recall of contextual information from prior time steps, which is critical for sequential modelling. It also increases non-linearity, enabling better representation of complex temporal patterns across various tasks. Thus, SST provides a broadly applicable activation choice to enhance sequential modelling, especially in data-constrained environments and thereby facilitates faster and more accurate learning.

In this article, the following main contributions are made:

1. SST, a new AF, is introduced to enhance the classical GRU performance when the dataset size is limited, and the pattern is sparse.
2. Distinct properties of typical AFs like non-linearity, boundedness, smooth gradients, and faster convergence are discussed.
3. Extensive empirical evaluation of SST-powered GRU across various applications involving time-series classification, sign language prediction, and speech recognition is presented.

2. Related works

Neural network architectures rely heavily on AFs, especially for complex tasks, to model non-linear patterns. The Sigmoid and TanH functions are widely used due to their smooth non-linear characteristics that recall biological neurons [15]. However, these functions encounter significant issues with saturation and vanishing gradients, which hinder learning in deep network

architectures. Rectified activations like ReLU [3] improve feedforward networks' performance by diminishing vanishing gradients. Following this, several variants of ReLU, including leaky ReLU [4], parametric ReLU [5], and exponential linear units (ELU) [11], were introduced to address some of the inherent drawbacks of the original ReLU function, such as the dying neuron problem. However, their application in sequential modelling remains challenging, particularly in RNNs, LSTMs, and GRUs [6-9, 16]. Recently, there are several AFs introduced for recurrent networks. Swish [17] employs a self-gating mechanism that blends linear and ReLU-like behaviours, while self-learnable functions [18] adaptively learn an ensemble of identity mappings as activations. These developments, although promising for feedforward networks, have not translated into substantial improvements in sequential tasks. In continuation, there are novel parameterized cells like simplified recurrent units (SRU) [19] and Quasi-RNN [20], indicating a trend towards recurrent architectures. However, a fundamental transformation in AFs for GRUs and LSTMs, which remain dominant in sequential data processing, is still relatively underexplored.

While there are efforts like adaptive piecewise linear units [21], which attempt to introduce specialized recurrent activations, these do not fully address the constraints posed by sequential data, particularly in scenarios involving sparse patterns under limited data. These limitations highlight a crucial gap in current approaches and underscore the need for AFs that are not only tailored to the unique requirements of recurrent architectures but also cater to the nuances of sequential data processing. Our work contributes to this area by proposing the SST AF, explicitly designed to enhance training and generalization in classical GRU, when dealing with small sequential datasets containing sparse patterns. SST squares the outputs of the Sigmoid and TanH functions, thereby augmenting gradient propagation and signal filtering, which is crucial for memory retention as signals evolve over time. This approach is directly targeted at mitigating the long-range dependency limitations inherent in existing activation schemes. Through our empirical studies, we demonstrate SST's effectiveness in enhancing classical GRU, providing new insights and empirical evidence for an open problem in neural network research.

3. Motivation and Intuition behind SST

In certain cases, the performance of a sequential model is inhibited by the limited dataset exhibiting sparse patterns. Sigmoid and TanH, with their saturation properties, can exacerbate the problem by squashing gradients during backpropagation, leading to diminished learning signals. This is particularly problematic in tasks with inherently sparse patterns in the datasets where the retention of every possible signal is crucial for effective learning. To visualize sparse patterns in the dataset, principal component analysis (PCA) is used on the Indian sign language (ISL) dataset [22], as shown in Figure 1. For this visualization, three distinctive sign classes (friend, phone call, location) were selected as representative examples. PCA visualizations highlight discernible clusters corresponding to each sign class. Each red point represents a feature extracted from sequential models. Pattern sparsity is evidenced by areas where red dots are widely dispersed. These sparse areas pose significant challenges for traditional AFs like Sigmoid and TanH in the learning process. They tend to either activate too strongly or not at all, causing a loss of gradient information that is critical for model training, particularly in the context of recognizing the subtleness of sign language. To overcome this obstacle, SST is introduced. SST enhances the model's sensitivity to sparse signals by amplifying the gradients of non-zero inputs, thereby ensuring that even subtle, less frequent gestures within the sign language spectrum are captured and learned effectively. This amplification is particularly advantageous in the sparse regions of the PCA plot, where traditional activations might fail to differentiate between the nuanced gestures that define a language as complex as ISL.

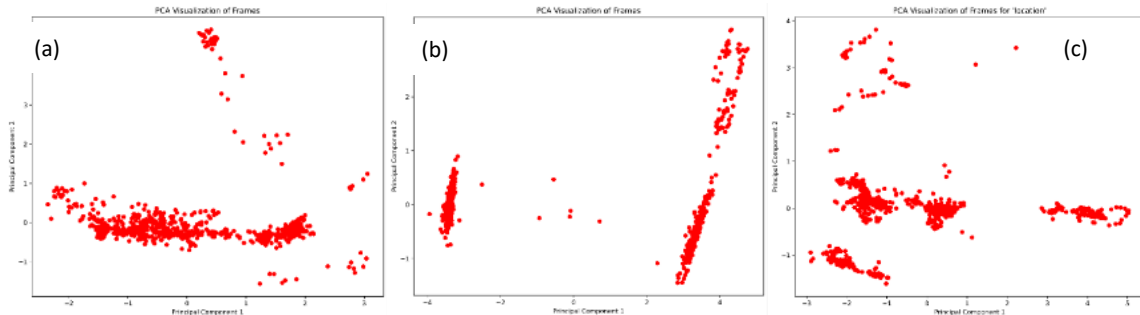


Fig.1 PCA visualization of frames for three distinct ISL classes - (a) friend, (b) phone call, and (c) location.

4. Squared Sigmoid TanH (SST)

Classical GRU plays a crucial role in addressing temporal dependencies, especially in modelling short-term and long-term sequences. A GRU cell contains two main components - a reset gate (r_t) and an update gate (z_t). These gates modulate the flow of information inside the GRU cell using Sigmoid activation, controlling whether to forget the previous state or consider the latest input. The output (h_t) is a linear interpolation between the previous activation (h_{t-1}) and the GRU's candidate activation (\tilde{h}_t) that processes the current input and previous state through a TanH layer. Although GRU exhibits a remarkable capacity to perform well in situations where training sequential data is limited [23], the classical GRU struggles to learn sparse pattern in the data and is unable to effectively propagate signals through time and layers [24]. To address this issue, a novel idea, SST is introduced. SST squares the output of Sigmoid function within the GRU layers and TanH Function in the dense layers, as these AFs are commonly

used in sequential modelling, as shown in Figure 2. The idea of SST is that, for instance, after squaring Sigmoid AF, the higher input probability value gets relatively higher than the lower input probability value. This approach enhances model learning efficiency and improves the accuracy of the neural network. In the following subsections, we discuss the properties of the squared Sigmoid and squared TanH AFs to formulate the SST.

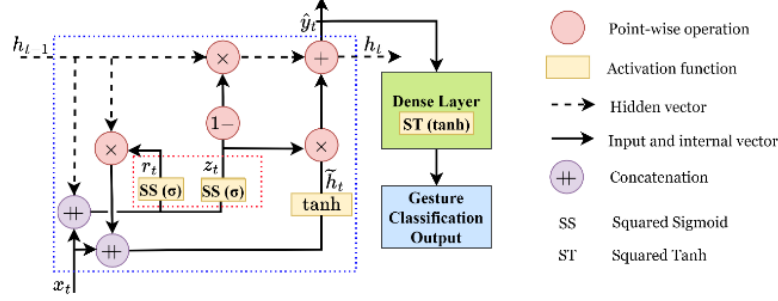


Figure 2. SST-AF in a GRU cell.

4.1 Squared sigmoid (SS)

The SS is achieved by squaring the generic Sigmoid function (SF). It is defined by

$$SS(x) = (SF(x))^2, \text{ where } SF(x) = \frac{1}{(1+e^{-x})}. \quad (1)$$

The behaviour of SF and SS is displayed in Figure 3(a). The typical SF results in [0,1]. When SS is applied, the higher output probability value of SF is retained relatively higher when compared to the lower value getting very small. For example, $(0.9)^2$ and $(0.1)^2$ result in 0.81 and 0.01, respectively. This suggests that neurons are activated to focus on the larger value in retaining the sparse patterns. To emphasize the applicability of SS as AF in sequential models, it is essential to discuss the basic properties of a generic AF. They are boundedness, non-linearity, continuity, and differentiability.

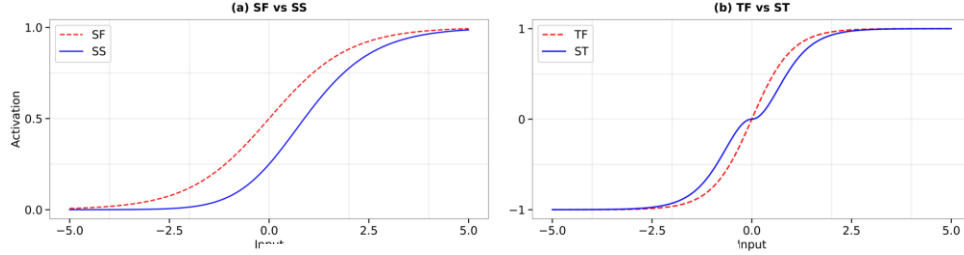


Figure 3. Behaviour of (a) SS and (b) ST

(a) Range: SS produces a similar S-shaped curve stretched between 0 and 1.

Proof: To find the range of $SS(x)$, we show that $\forall x \in \mathbb{R}, 0 \leq SS(x) \leq 1$. Since SF is bounded by [0,1], squaring both sides results in [0,1], stretching the curve.

(b) Non-linearity: SS introduces more nonlinearity to the model than the traditional SF .

Proof: Rate of change of SS is a function. When $\frac{d}{dx} SS(x)$ is taken, it results in $2 * SF(x)$, which is nonlinear, as shown in Figure 3(a). Hence, the SS has a more pronounced curvature in the middle of the curve compared to the SF . It means that it can map more complex sparse patterns in the data, as SS is more sensitive to small changes in the input.

(c) Continuity: SS is continuous at all points in the curve.

Proof: To prove $SS(x)$ is continuous, we consider the composition rule of continuity which states that if $g(x)$ is continuous at $x = a$ and $h(x)$ is continuous at $x = g(a)$, then the composite function $f(x) = g(h(x))$ is also continuous at $x = a$. In our case, we apply the composition rule to $g(x) = x^2$ and $h(x) = SF(x)$ to show that $SS(x) = g(h(x))$ is continuous. We know that $\forall x, h(x)$ and $g(x)$ are continuous. Therefore, by the composition rule for continuity, $\forall x, SS(x) = g(h(x)) = x^2 * (SF(x))^2$ is also continuous.

(d) Differentiability: SS is differentiable.

Proof: To prove $SS(x)$ is differentiable $\forall x$, we show that there exists derivative at every point in its domain. Using the chain rule and the derivative of the logistic function, we find the derivative of SF and SS as follows

$$SF'(x) = SF(x) * (1 - SF(x)). \quad (2)$$

$$SS'(x) = 2 * SF(x) * SF'(x). \quad (3)$$

Substituting Eq. (2) in Eq. (3), we get

$$SS'(x) = 2 * SF(x) * (1 - SF(x)) * SF(x) = 2 * (SF(x))^2 * (1 - SF(x)). \quad (4)$$

Since SF is differentiable $\forall x$, the product of two differentiable functions is differentiable. Therefore, SS is also differentiable $\forall x$ in its domain.

4.2 Squared TanH (ST)

ST is obtained by squaring the classical hyperbolic tangent function (TF) and mathematically defined by

$$ST(x) = \begin{cases} -(TF(x))^2, & \text{if } x < 0 \\ (TF(x))^2, & \text{if } x \geq 0 \end{cases}, \text{ where } TF(x) = \frac{e^x - e^{-x}}{e^x + e^{-x}}. \quad (5)$$

Here, squaring the -ve value is returned as -ve of the squared value, as given in Eq. (5). Otherwise, the behaviour of ST is not adhered to the classical TF . The behaviour of TF and ST is shown in Figure 3(b), in which ST displays much higher non-linearity away from the origin. As TF is modified, we discuss how it impacts and ensures the properties of typical AFs.

(a) Range: ST has a similar S-shaped curve like TF but with a narrow waist in the middle, as shown in Figure 3(b) and it is bounded to $[-1,1]$.

Proof: To prove the boundedness of ST outcome $[-1, 1] \forall x, x \in \mathbb{R}$, consider the following two cases.

- For $x \geq 0$, since $TF(x)$ ranges $[0, 1]$, $(TF(x))^2$ also ranges $[0, 1]$.
- For $x < 0$, since $TF(x)$ ranges $[-1, 0)$, we use $-(TF(x))^2$ which ranges $[-1, 0)$.

Combining these cases together, Eq. (5) is bounded $[-1, 1] \forall x, x \in \mathbb{R}$.

(b) Non-linearity: ST is non-linear.

Proof: To prove ST is non-linear, we must show that it does not satisfy the property of additivity. It means that $ST(a + b) \neq ST(a) + ST(b)$. For given $a, b \in \mathbb{R}$, non-linearity is obvious for ST when $a, b \geq 0$. Therefore, we provide a clarity on non-linearity for ST when $a, b < 0$. From Eq. (5), we get $ST(a + b) = -(TF(a + b))^2$ when $a + b < 0$. To prove non-linearity, the following inequality holds $-(TF(a + b))^2 \neq -(TF(a) + TF(b))^2$. Hence, additivity property is not applicable for the two cases considered above.

(c) Continuity: ST is continuous.

Proof: To prove ST is continuous, it is sufficient to show that the ST is continuous at $x = 0$. Consider the limit of $ST(x)$ as x approaches 0 from the left and right direction on real number line.

$$\text{For } x \in \mathbb{R}^-, \lim_{x \rightarrow 0} -(TF(x))^2 = \lim_{x \rightarrow 0} -(0)^2 = 0$$

$$\text{For } x \in \mathbb{R}^+, \lim_{x \rightarrow 0} (TF(x))^2 = \lim_{x \rightarrow 0} (0)^2 = 0$$

Since both the left and right limits are equal to 0, we can conclude that the ST is continuous at $x = 0$.

(d) Differentiability: ST is differentiable.

Proof: To show that ST is differentiable at any \mathbb{R} , let us consider the chain rule, which rule states that if there is a composite function $f(g(x))$, then the derivative of $f(g(x))$ is given by $f'(g(x)) * g'(x)$. Let $f(x) = TF(x)$ and let $h(x) = 2I(x) - 1$, where $I(x)$ is the indicator function. Then the ST can be expressed as

$$g(x) = f(x)^2 * h(x)$$

and the derivative of $g(x)$ is given by

$$g'(x) = 2f(x)f'(x)h(x) + f(x)^2h'(x). \quad (6)$$

Using the fact that $f'(x) = \text{Sec}^2(x)$, $h(x)$ is a piecewise constant and $h'(x)$ is 0 almost everywhere (except at $x = 0$), we simplify Eq. (6) as

$$g'(x) = 2TF(x) \text{Sec}^2(x) [2I(x) - 1], \text{ if } x \neq 0$$

It turns out that $g(0) = 0$. Note that $\text{Sec}^2(x)$ and $2I(x) - 1$ are both continuous functions at any \mathbb{R} , so their product is also continuous at any \mathbb{R} . Thus ST is differentiable at any \mathbb{R} , except possibly at $x = 0$, where we have a corner point.

4.3 SST (SS+ST)

To improve the performance of the classical GRU, the SST is conceived based on observing and understanding their role in the gating mechanism, as well as their properties discussed in the previous sections. The basic concept of the SST is that to make the small values even smaller and the large values even larger, by squaring the output of SF in r_t and z_t , and TF in the dense layers, such that SST

- boosts gradient flow, resulting in faster and accurate learning.
- enhances the memory retention capability of the GRU cell and helps better recall information from previous t.
- provides a greater degree of non-linearity, which is particularly important for r_t to capture complex patterns and determine what information should be retained.

- emphasizes the robustness of GRU cells to noise input values by focusing on important information, particularly for z_t , which determines how much of h_{t-1} to retain.

It is important to observe that we did not replace the default TF in \tilde{h}_t of the GRU, as it can make it difficult to update \tilde{h}_t over time. Also, the reason for not using the widely used ReLU AF in the dense layer is to avoid the “zero-gradient” problem for the negative inputs and to provide smooth gradient transitions to improve the overall stability and convergence rate of the neural network. Eventhough ReLU has been shown to work well in many cases, the use of ST in the dense layers was superior to ReLU in terms of test accuracy. Ultimately, as expected, SST improved the overall performance and learning efficiency of the neural networks.

5. Experiments

We comprehensively analyse the effectiveness of SST compared to traditional functions (Sigmoid and TanH) on different tasks, such as sign language recognition, regression, gait classification and human activity recognition tasks. The simulation employed Python 3.7 on a desktop system featuring 32 GB RAM and an Intel Core i7 processor with a clock speed of 3.60 GHz. The operating system used was Windows 10 Pro (64-bit).

5.1 Sign Language Recognition

Sign language recognition is a critical task in human-computer interaction, enabling seamless communication with individuals who are deaf. For the experiments, the configuration is set according to [22]. The authors employ mediapipe optimized gated recurrent unit (MOPGRU) model to improve the performance with limited datasets. It consisted of real-time video recordings of 13 distinct Indian sign gestures as mentioned in [22]. Each sign gesture was represented by a collection of 30 videos, each comprising 30 frames, and all videos shared a uniform size of 640×480 pixels. To understand the data better, PCA visualization tool was adopted. From the plot, we observed that there exists sparse pattern in the ISL data as shown in Figure 1. To address data sparsity, enhance the accuracy of the MOPGRU model and to prove the power of SST AF further, SST AF has been incorporated into the MOPGRU model, resulting in the MOPGRU-SST configuration. The performance of MOPGRU-SST is compared against the baseline MOPGRU model, and the results will be discussed in the following section.

Confusion Matrix Analysis: The confusion matrix as shown in Figure 4 provides a comprehensive overview of the model's classification performance, comparing the actual versus predicted classifications. In the figure, columns represent the predicted labels while rows stand for the true labels for 13 ISL gesture classes. The numbers within each cell indicate the count of samples in the test set for that class. According to Figure 4(a), the confusion matrix resulting from the MOPGRU model shows a distinct pattern, with certain categories predicted with a high level of accuracy as well as significant challenges in differentiating between various classes because of possible underlying similarities. However, it is noteworthy that Figure 4(b) the confusion matrix of the MOPGRU-SST model, which is characterized by dark diagonal cells, suggesting a high percentage of true positives. This consolidated view emphasizes SST AF's unique strengths in the data-sparse classification landscape.

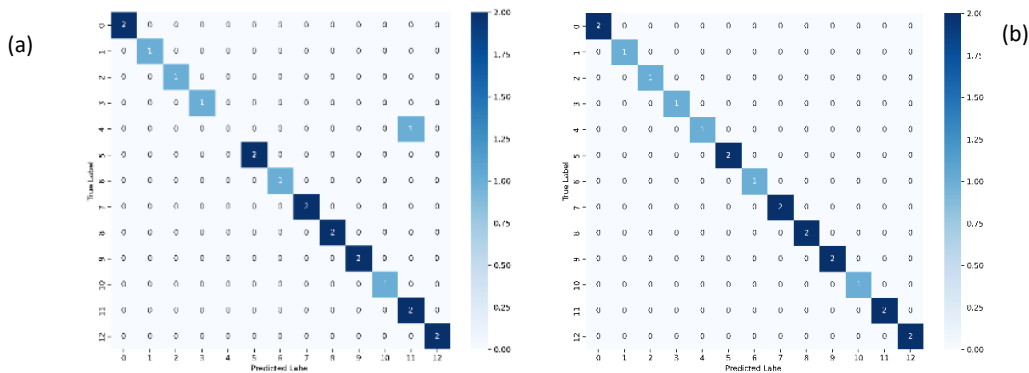


Fig.4 Comparative Confusion Matrices of (a) MOPGRU, and (b) MOPGRU-SST Models.

Visualization Insights of SST using T-SNE in neural network: The visualization of hidden layer outputs as shown in Figure 5(a) and (b) offers a compelling view into the semantic representation capabilities of the MOPGRU and MOPGRU-SST models. In the t-SNE plots, we observe that MOPGRU forms broader clusters for words such as "think," "phone call," and "meet," which could be indicative of its capacity to capture and represent semantic relationships. In contrast the separation is more prominent in MOPGRU-SST, signifying its ability to encode knowledge representations in a highly distinguished, nuanced manner. This differentiation can enhance recognition capabilities by efficiently mapping varying inputs to more granular model concepts. Analysing the dense layer visuals reveals similar insights, with MOPGRU-SST in Figure 6(a) producing clearer delineation between clusters representing different terms. The evident distinction of semantic groupings compared to MOPGRU in Figure 6(b)

indicates that MOPGRU-SST develops richer hierarchical data representations. Overall, by comparing the test accuracy of both models, MOPGRU-SST achieved a higher accuracy of 100% than baseline MOPGRU which achieved 95%.

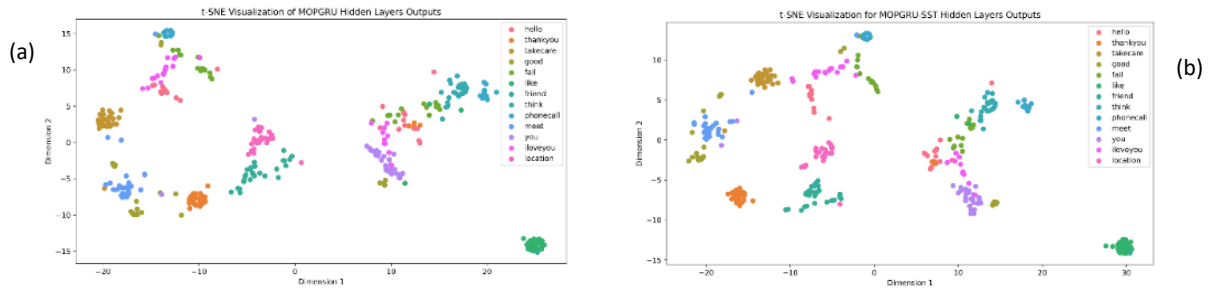


Fig.5 T-SNE visualization of hidden layer outputs: (a) MOPGRU, and (b) MOPGRU-SST Models.

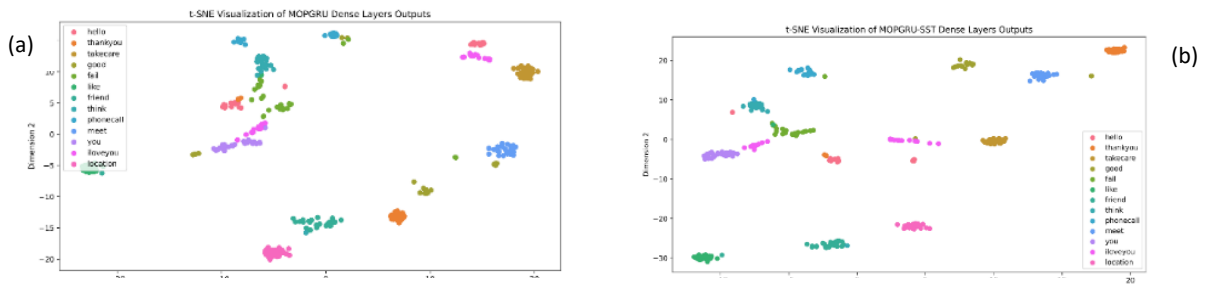


Fig.6 T-SNE visualization of dense layer outputs: (a) MOPGRU, and (b) MOPGRU-SST Models.

5.2 Gait classification

We utilize an accelerometer-based gait dataset from [26] comprising raw acceleration sequences collected from 244 subjects during a 3-minute walking task. The dataset provides a robust test application for evaluating recurrent models for classifying dynamic human activities that are sequential in nature. The original dataset, although suitable for analysing age-related differences in gait patterns as explored in [26], does not contain sparsity to specifically assess model resilience within data constraints. Since real-world sensor feeds often encounter missing information, we introduce sparsity to simulate this practical challenge. Specifically, 20% of values in the 1024-sample input sequences were randomly zeroed out to induce missing data points across temporal dimensions. Figure 7 depicts the data distribution before and after sparsity injection. In the induced sparse dataset, a sharp peak at zero indicates significant conversion of values to a single number, effectively creating sparse sequences. With 1460 sequences originally, this process generates 1168 non-sparse and 292 sparse patterns in the final training dataset. The incorporation of sparse data simulations allows comprehensive benchmarking of SST-powered GRU models against traditional GRUs in handling sparse temporal inputs. Training the model, the experimental setup and model training parameters follow the same as mentioned in [26] with the additional incorporation of SST AF in the classical GRU. For evaluating the classification performance, widely used evaluation metrics such as accuracy, precision, recall and F1 score were used. In addition, receiver operating characteristic (ROC) curves were generated and the area under the curve (AUC) was calculated which will be discussed in detail below.

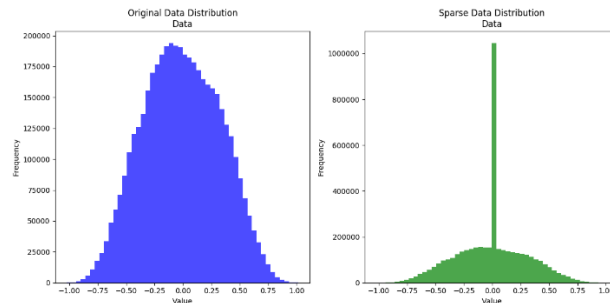


Fig.7 Comparative Histograms of Feature Value Distributions: Original (left) vs. Induced Sparsity (right) in Dataset

Classification performance: The integration of the proposed SST activation consistently improves GRU performance over the baseline across evaluation metrics as observed in Table 1. GRU-SST achieves a superior test accuracy of 84.3% compared to

classical GRU's 79.8%. Precision increases from 78.9% to 87.7% with SST incorporation. Further, GRU-SST obtains an AUC of 0.92, substantially superior to the baseline GRU's 0.86 AUC - indicating higher discrimination between classes. With consistent gains in accuracy, precision, recall, and AUC, SST demonstrates concrete effectiveness in addressing GRU limitations when learning from

Tab. 1 The performance metrics of GRU and GRU-SST

| Model | Test Accuracy | Precision | Recall | F1-score | AUC |
|---------|---------------|--------------|--------|--------------|-------------|
| GRU | 79.8% | 78.9% | 77.8% | 78.3% | 0.86 |
| GRU-SST | 84.3% | 87.7% | 77.4% | 82.2% | 0.92 |

sparse temporal data. The results validate SST's strengths in transforming classical recurrent models within constraints to boost predictive performance.

ROC and AUC curve analysis: The ROC curve shown in Figure 8 illustrates the performance of baseline GRU and GRU-SST models on a classification task. The red line represents the true positive rate (TPR) versus the false positive rate (FPR) at various threshold levels. An ideal model would have a curve that reaches towards the top left corner, indicating a high TPR and low FPR. The ROC analysis provides evidence on SST's efficacy with GRU-SST producing a higher AUC of 0.92 over the baseline's 0.86. This increased AUC value from 0.86 to 0.92 signifies a notable improvement in model performance, highlighting the potential of SST to improve the robustness and predictive accuracy of GRU networks in classification-ROC curve results.

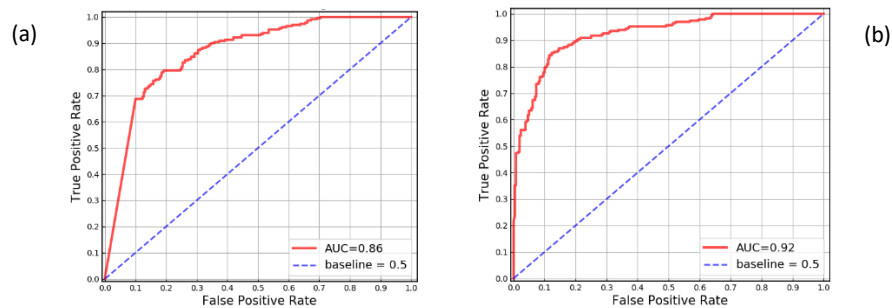


Fig. 8 ROC curve for (a) GRU and (b) GRU-SST

Error analysis using confusion matrix: The confusion matrices in Figure 9 compare model behaviours and misclassification trends. While the baseline GRU model attains decent performance across both classes (79.8% overall accuracy), incorporation of SST enhances predictive capability further. GRU-SST achieves a considerably higher overall accuracy of 84.3%, driven by appreciable gains within the adult class (90.4% true positives vs 81.5% for GRU). The false negative rate for misclassifying Adults drops noticeably from 18.5% to 9.6% with SST. Though the false positive rate classifying Older Adults shows a minor increase (22.6% vs 22.2% in GRU), GRU-SST exhibits more balanced classification overall - validating SST's effectiveness despite data sparsity. Overall SST demonstrates clear and consistent effectiveness across metrics in addressing GRU limitations on scarce data - significantly elevating classification accuracy through enhanced gradient flows and re-calibration of gates.

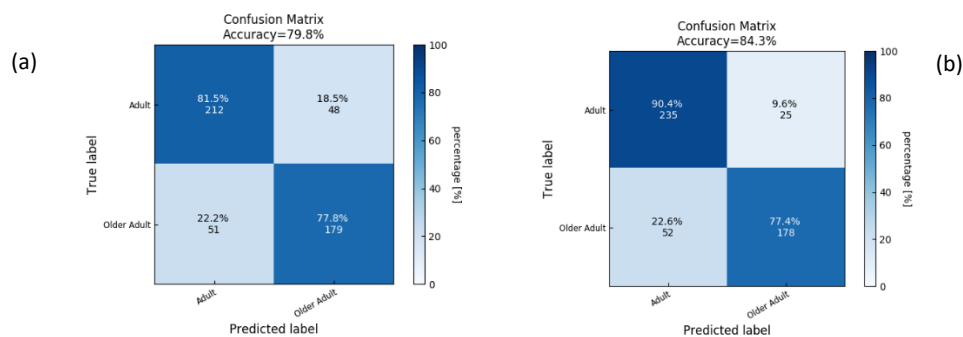


Fig. 9 Confusion matrix for (a) GRU and (b) GRU-SST

5.3 Human activity recognition

Human activity recognition (HAR) using wearable sensors provides an attractive test application for evaluating sequential modelling techniques. Sensor feeds capturing motions over time exhibit temporal dependencies well-suited to GRU networks. We leverage two standard HAR datasets to evaluate our proposed SST activation in enhancing GRU models. The first is the WISDM dataset [27] comprising 1,098,207 samples from 36 subjects performing daily activities like walking, jogging, sitting, and standing. The second is the UCI Smartphone dataset [28] containing 10,299 instances of sensor readings from 30 volunteers aged 19 to 48 years executing 6 standard activities - standing, sitting, lying, walking, upstairs and downstairs using a mobile phone. Each subject performed the protocol twice with varying device placements. 50Hz triaxial acceleration and angular velocity data were recorded and manually labelled. We induced 20% sparsity into both datasets to simulate real-world sensor feed challenges. For training, we followed [29] and compared classical GRU and GRU-SST performance for both datasets. The comparative evaluation results summarized in Table 2 clearly validate the effectiveness of the proposed SST activation in enhancing classical GRU models for human activity recognition, consistently across both datasets.

Tab. 2 Comparative Performance of GRU and GRU-SST Models on WISDM and UCI-HAR Datasets

| Model | Dataset | Training Accuracy (%) | Testing Accuracy (%) |
|---------|---------|-----------------------|----------------------|
| GRU | WISDM | 99.5 | 97.08 |
| GRU-SST | WISDM | 100 | 99.28 |
| GRU | UCI-HAR | 99 | 93.08 |
| GRU-SST | UCI-HAR | 100 | 98.30 |

On sparse WISDM accelerometer data, SST allows GRU models to achieve near to 100% training accuracy. More importantly, test accuracy increases over 2% with GRU-SST, reaching 99.28% despite introduced sparsity. Similarly on Smartphone data, SST again shows generalization capability improving GRU test accuracy by 5% to 98.3%. The results validate SST's effectiveness in tackling GRU limitations on multivariate time series across application domains. By reshaping classical activations, SST unlocks substantial accuracy and convergence gains.

5.4 Time-series forecasting

In financial forecasting, the ability to accurately predict future prices of commodities like gold is a testament to a model's predictive prowess. Gold, a commodity of high economic interest, presents a challenging yet valuable dataset for time series analysis. The historical gold price dataset from Yahoo Finance, with its comprehensive range of data points from 2000 to 2023, was chosen for its complexity and relevance. The dataset's granular details, including open, high, low, close, and adjusted close prices, offer a multifaceted view of market behaviour, allowing the model to learn from sparse temporal patterns. The choice to use this dataset aligns with our objective to assess SST's ability to enhance GRU model performance. The daily fluctuations and trends encapsulated within gold price data require a model that discerns long-term dependencies. SST's design to amplify gradient flow and improve information retention is put to the test, making this dataset suitable for demonstrating SST's potential to refine predictions in a complex and unpredictable domain like financial time series. For training, we utilized the model configuration from [30] based on GRU architecture by replacing the LSTM layers. To analyze SST improvements, mean squared error (MSE) loss was calculated between predicted and ground truth gold prices over the test period. As evidenced in Table 3, SST integration leads to substantial reductions in error metrics consistently across training and validation. GRU-SST lowers MSE compared to baseline GRU in terms of training and validation loss by over 20%. The test set MSE declines even further from 0.28 to 0.08. These consistent MSE reductions across phases validate SST's capability in accurately modelling temporal dependencies for financial forecasting with GRUs. By tuning activations to sequential data, SST unlocks substantial predictive performance gains over classical approaches.

Tab.3 Loss and MSE Comparison for GRU and GRU-SST on Gold Price Forecasting

| Model | Training Loss | Validation Loss | MSE |
|---------|---------------|-----------------|------|
| GRU | 0.70 | 0.08 | 0.28 |
| GRU-SST | 0.54 | 0.06 | 0.08 |

6. Conclusion

This study presents the Squared Sigmoid TanH (SST) activation function, designed to improve GRU models' performance in sparse data environments, especially when the dataset is limited. The performance of SST has been demonstrated across a variety of sequential tasks. In sign language recognition, the SST-enhanced GRU model achieved an impressive 100% test accuracy, a significant leap from the baseline. For gait classification, it again outperformed the standard GRU, registering a test accuracy of 84.3% compared to the baseline's 79.8%. For human activity recognition, the SST implementation resulted in near-perfect training accuracy and increased test accuracy by over 2.2%, reaching 99.28%. Similarly, SST improved GRU's test accuracy by 5%, achieving

98.3% on the Smartphone data. Additionally, SST's integration significantly reduced the MSE in gold price prediction to 0.08 from 0.28, as well as both training and validation losses, suggesting that it has a substantial impact on forecasting accuracy. This study demonstrates SST's ability to accurately model complex temporal dependencies and its effectiveness in real-world applications, adding significant value to deep learning.

References

1. W.Duch,N. Jankowski, Survey of neural transfer functions, *Neural Computing Surveys*2(1)(1999)163–212.
2. LeCun, Y., Bengio, Y. & Hinton, G. Deep learning. *Nature* 521, 436–444 (2015).
3. V.Nair,G.E.Hinton, Rectified linear units improve restricted boltzmann machines, *International Conference on Machine Learning*, 2010, pp. 807–814.
4. A.L.Maas, A.Y.Hannun, A.Y.Ng, Rectifier nonlinearities improve neural network acoustic models, *International Conference on Machine Learning*, Vol.30,2013, p.3.
5. K.He, X.Zhang, S.Ren, J.Sun, Delving deep into rectifiers: Surpassing human-level performance on ImageNet classification, *IEEE international conference on computer vision*, 2015, pp.1026–1034.
6. Pascanu, Razvan, Tomas Mikolov and Yoshua Bengio. "On the difficulty of training recurrent neural networks." *International Conference on Machine Learning* (2012).
7. S. Hochreiter and J. Schmidhuber, "Long Short-Term Memory," in *Neural Computation*, vol. 9, no. 8, pp. 1735-1780, 15 Nov. 1997, doi: 10.1162/neco.1997.9.8.1735.
8. Cho K, van Merriënboer B, Gulcehre C, Bougares F, Schwenk H, Bengio Y. Learning phrase representations using RNN encoder-decoder for statistical machine translation. In *Conference on Empirical Methods in Natural Language Processing (EMNLP 2014)*. 2014
9. Gers, Felix Alexander, Jürgen Schmidhuber and Fred Cummins. "Learning to Forget: Continual Prediction with LSTM." *Neural Computation* 12 (2000): 2451-2471.
10. John F. Kolen; Stefan C. Kremer, "Gradient Flow in Recurrent Nets: The Difficulty of Learning Long Term Dependencies," in *A Field Guide to Dynamical Recurrent Networks*, IEEE, 2001, pp.237-243, doi: 10.1109/9780470544037.ch14.
11. D.-A.Clevert, T.Unterthiner, S.Hochreiter, Fast and accurate deep network learning by exponential linear units(elus), *InternationalConferenceonLearningRepresentations*,2016.
12. Bengio, Yoshua, Patrice Simard, and Paolo Frasconi. "Learning long-term dependencies with gradient descent is difficult." *IEEE transactions on neural networks* 5.2 (1994): 157-166.
13. Glorot, Xavier, Antoine Bordes, and Yoshua Bengio. "Deep sparse rectifier neural networks." *Proceedings of the fourteenth international conference on artificial intelligence and statistics. JMLR Workshop and Conference Proceedings*, 2011.
14. Amodei, Dario, et al. "Deep speech 2: End-to-end speech recognition in english and mandarin." *International conference on machine learning*. PMLR, 2016.
15. Cybenko, G. (1989). "Approximation by superpositions of a sigmoidal function." *Mathematics of control, signals, and systems*, 2(4), 303-314.
16. Fadziso, Takudzwa. "Overcoming the Vanishing Gradient Problem during Learning Recurrent Neural Nets (RNN)." *Asian Journal of Applied Science and Engineering* (2020).
17. Ramachandran, Prajit, Barret Zoph and Quoc V. Le. "Searching for Activation Functions." *ArXiv abs/1710.05941* (2018).
18. Goyal, Mohit, Rajan Goyal and Brijesh Lall. "Learning Activation Functions: A new paradigm of understanding Neural Networks." *ArXiv abs/1906.09529* (2019).
19. Lei, Tao, Yu Zhang and Yoav Artzi. "Training RNNs as Fast as CNNs." *ArXiv abs/1709.02755* (2017).
20. Bradbury, James, Stephen Merity, Caiming Xiong and Richard Socher. "Quasi-Recurrent Neural Networks." *ArXiv abs/1611.01576* (2016).
21. Agostinelli, F., et al. (2015). "Learning activation functions to improve deep neural networks." *ICLR Workshop*.
22. Subramanian, B., Olimov, B., Naik, S.M. et al. An integrated mediapipe-optimized GRU model for Indian sign language recognition. *Sci Rep* 12, 11964 (2022).
23. B. Verma, "A two stream convolutional neural network with bi-directional GRU model to classify dynamic hand gesture," *J. Vis. Commun. Image Represent.*, vol. 87, no. April, p. 103554, 2022.
24. Semeniuta, Stanislaw, Aliaksei Severyn, and Erhardt Barth. "Recurrent dropout without memory loss." *arXiv preprint arXiv:1603.05118* (2016).
25. D. Harrison and D. L. Rubinfeld, "Hedonic housing prices and the demand for clean air," *J. Environ. Econ. Manage.*, vol. 5, no. 1, pp. 81–102, 1978.

26. Zheng, Xiaoping et al. "Explaining Deep Learning Models for Age-related Gait Classification based on time series acceleration." ArXiv abs/2311.12089 (2023).
27. Jennifer R. Kwapisz, Gary M. Weiss, Samuel A. Moore, Activity Recognition using Cell Phone Accelerometers. SigKDD Explorations, Volume 12, Issue 2, 2010.
28. Davide Anguita, Alessandro Ghio, Luca Oneto, Xavier Parra and Jorge L. Reyes-Ortiz. A Public Domain Dataset for Human Activity Recognition Using Smartphones. 21th European Symposium on Artificial Neural Networks, Computational Intelligence and Machine Learning, ESANN 2013. Bruges, Belgium 24-26 April 2013.
29. Mohsen, S. Recognition of human activity using GRU deep learning algorithm. Multimed Tools Appl 82, 47733–47749 (2023).
30. W. M. P. Dhuhita, M. F. A. Farid, A. Yaqin, H. Haryoko and A. A. Huda, "Gold Price Prediction Based On Yahoo Finance Data Using Lstm Algorithm," 2023 International Conference on Informatics, Multimedia, Cyber and Informations System (ICIMCIS), Jakarta Selatan, Indonesia, 2023, pp. 420-425.